AD-A164 358   EFFECTS OF VARIATION OF INDEX OF REFRACTION OF   1/1
ATMOSPHERE ON CERENKOV RADIATION(U) NAVAL POSTGRADUATE
SCHOOL MONTEREY CA   K R JOO DEC 85
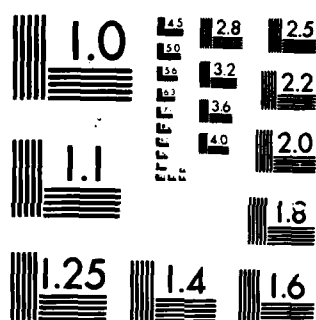
UNCLASSIFIED   F/G 20/8   NL

END
FILMED
3-86
DTIC

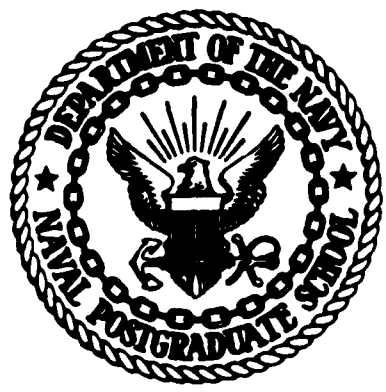|					
	1.0		2.8	2.5	
			3.2	2.2	
			3.6		
	1.1		4.0	2.0	
				1.8	
	1.25	1.4		1.6	

MICROCOPY RESOLUTION TEST CHART
NATIONAL BUREAU OF STANDARDS-1963-A

NAVAL POSTGRADUATE SCHOOL
Monterey, California

DTIC
ELECTE
S
FEB 1 4 1986
D
B

THESIS

EFFECTS OF VARIATION OF INDEX OF REFRACTION OF

ATMOSPHERE ON CERENKOV RADIATION

by

Joo, Kyung Ro

December 1985

Thesis Advisor: John R. Neighbours

Approved for public release; distribution is unlimited.

86 2 14 072

AD-A164 356

REPORT DOCUMENTATION PAGE

1a. REPORT SECURITY CLASSIFICATION UNCLASSIFIED		1b. RESTRICTIVE MARKINGS		
2a. SECURITY CLASSIFICATION AUTHORITY		3. DISTRIBUTION / AVAILABILITY OF REPORT		
2b. DECLASSIFICATION / DOWNGRADING SCHEDULE		Approved for public release; distribution is unlimited.		
4. PERFORMING ORGANIZATION REPORT NUMBER(S)		5. MONITORING ORGANIZATION REPORT NUMBER(S)		
6a. NAME OF PERFORMING ORGANIZATION Naval Postgraduate School	6b. OFFICE SYMBOL (If applicable) 61	7a. NAME OF MONITORING ORGANIZATION Naval Postgraduate School		
6c. ADDRESS (City, State, and ZIP Code) Monterey, California 93943-5100		7b. ADDRESS (City, State, and ZIP Code) Monterey, California 93943-5100		
8a. NAME OF FUNDING / SPONSORING ORGANIZATION	8b. OFFICE SYMBOL (If applicable)	9. PROCUREMENT INSTRUMENT IDENTIFICATION NUMBER		
8c. ADDRESS (City, State, and ZIP Code)		10. SOURCE OF FUNDING NUMBERS		
		PROGRAM ELEMENT NO.	PROJECT NO.	TASK NO.	WORK UNIT ACCESSION NO.

11. TITLE (Include Security Classification)

Effects of Variation of Index of Refraction of Atmosphere on Cerenkov Radiation

12. PERSONAL AUTHOR(S)

Joo, Kyung Ro

13a. TYPE OF REPORT Master's Thesis	13b. TIME COVERED FROM _____ TO _____	14. DATE OF REPORT (Year, Month, Day) 1985 December	15. PAGE COUNT 48

16. SUPPLEMENTARY NOTATION

17.	COSATI CODES		18. SUBJECT TERMS (Continue on reverse if necessary and identify by block number)
FIELD	GROUP	SUB-GROUP	Index of refraction, Cerenkov radiation, Emission threshold

19. ABSTRACT (Continue on reverse if necessary and identify by block number)

Cerenkov radiation is calculated for electron beams which exceed the velocity of light in a nondispersive dielectric medium. The electron beam is assumed to be bunched as emitted from a travelling wave accelerator and the emission region is assumed to be finite.

The direction of emission of the Cerenkov radiation is related to the index of refraction which in turn is related to atmospheric index of refraction. The calculated index of refraction in the atmosphere predicts changes to the Cerenkov radiation pattern and the emission threshold condition.

20. DISTRIBUTION / AVAILABILITY OF ABSTRACT ☒ UNCLASSIFIED/UNLIMITED ☐ SAME AS RPT ☐ DTIC USERS	21. ABSTRACT SECURITY CLASSIFICATION Unclassified	
22a. NAME OF RESPONSIBLE INDIVIDUAL John R. Neighbours	22b. TELEPHONE (Include Area Code) (408) 646-2922	22c. OFFICE SYMBOL 61Nb

DD FORM 1473, 84 MAR   83 APR edition may be used until exhausted   SECURITY CLASSIFICATION OF THIS PAGE
All other editions are obsolete

Effects of Variation of Index of Refraction
of Atmosphere on Cerenkov Radiation

by

Kyung Ro Joo
Major, Korea Army
B.S., Dong-a University, 1982

Submitted in partial fulfillment of the
requirements for the degree of

MASTER OF SCIENCE IN ENGINEERING SCIENCE

from the

NAVAL POSTGRADUATE SCHOOL
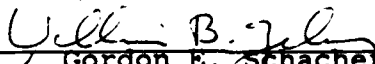December 1985

Author: _____
Kyung Ro Joo

Approved by: _____
John R. Neighbours, Thesis Advisor

_____
Fred R. Buskirk, Second Reader

_____
Gordon E. Schacher, Chairman,
Department of Physics

_____
John N. Dyer,
Dean of Science and Engineering

2

ABSTRACT

Cerenkov radiation is calculated for electron beams which exceed the velocity of light in a nondispersive dielectric medium. The electron beam is assumed to be bunched as emitted from a travelling wave accelerator and the emission region is assumed to be finite.

The direction of emission of the Cerenkov radiation is related to the index of refraction which in turn is related to atmospheric index of refraction. The calculated index of refraction in the atmosphere predicts changes to the Cerenkov radiation pattern and the emission threshold condition.

TABLE OF CONTENTS

4

LIST OF TABLES

LIST OF FIGURES

ACKNOWLEDGEMENTS

I would like to express my deep appreciation to Professor John R. Neighbours and Profssor Fred R. Buskirk for guidance, advice and corrections throughout this thesis.

Thanks also to my wife Young-ok and two sons Yong and Ho for support and understanding during my stay at U.S. Naval Postgraduate School. Special thanks to God.

I. INTRODUCTION

Cerenkov radiation is the radiation produced by a charge or group of charges, moving at speeds greater than light in a particular medium. It has been investigated, starting with the experiments of Cerenkov in 1934 and described in terms of a charged particle moving faster than the velocity of light in a medium by Frank and Tamm in 1937. A summary of work to 1958 is contained in the book by Jelley [Ref. 1].

The concept of Cerenkov radiation has been used occasionally as a detector of high speed charged particles. A detector using this concept will selectively detect only charged particles exceeding the velocity of light in the medium through which they are traveling. Other than this application to particle detection, it has been considered as a curiosity, and the phenomenon has been usually thought to be a weak source of broadband radiation.

Until recently the study of Cerenkov radiation has been restricted almost exclusively to radition in the optical region, and most theoretical and experimental studies have been devoted to the properties of Cerenkov radition in the optical band.

The Cerenkov angle is defined by $\cos\theta = c/v = 1/n\beta$, where c is the velocity of light in the medium, v is the velocity of the charged particle, n is the index of refraction, and β is the usual notation for the ratio of v to c_{e} where c_{e} is the velocity of light in vacumm. The term refraction in atmosphere is used to describe the capability of the atmosphere to bend an electro magnetic wave toward the region of higher refractive index. When conditions correspond to the standard atmosphere, a wave initially horizontal does not travel along a straight path but moves on a path bent slightly downward, but still not equal to the curvature of the earth except in unusual circumstances.

8

The atmospheric index of refraction is a function of temperature, pressure, and humidity [Ref. 2].

The purpose of this thesis is to understand how the Cenrenkov radiation produced by a charged particle beam propagating in air is affected by the the changes of index of refraction of the atmosphere. The atmospheric density range considered is appropriate for a range in altitude from sea level to 10 Km.

II. <u>THEORY</u>

A. CHARACTERISTICS OF CERENKOV RADIATION

A charged particle or a charge bunch in uniform motion in a straight line in free space does not radiate. The situation may be different, however, in a dielectric medium for which $k > k_0$, $\varepsilon > 1$, and index of refraction of the medium, n, can be written as:

$$n = \left(\frac{k}{k_0}\right)^{\frac{1}{2}} = [\varepsilon]^{\frac{1}{2}} \qquad \text{(eqn 2.1)}$$

where k_0 is a permittivity of free space, k is a permittivity of medium, and ε is a dielectric constant of the medium.

If the charge is moving fast, that is, at a velocity greater than that of light in the medium, a dipole field results which will be apparent even at large distances from the track. Such a field will be momentarily set up by the charge bunch at each line element along the track, and in turn each molecule in the line element will then radiate a brief electromagnetic pulse. The radiation will be spread over a band of frequencies corresponding to the various Fourier componts of this pulse.

In the general case, the radiated wavelets from all parts of the track interfere destructively so that, at a distant point, the resultant field intensity is still zero. However, if the velocity of the particle is greater then the phase velocity of the radiated wave in the medium, it is possible for the wavelets from all portions of the track to be in phase with one another so that, at a distant point of observation, there is now a resultant radiation field.

Figure 2.1   Huygens Construction of Wavelet
for   Cerenkov Radiation.

It will be understood from the Huygens construction shown in figure 2.1 that this radiation is only observed at a particular angle θ_c with respect to the track of the particle, namely that angle at which the wavelets from arbitary points such as p1, p2 and p3 on the track AB are coherent and combine to form a plane wave front, BC. This coherence takes place when the particle traverses AB in the same time that the light wave travels from A to C. If β is defined as v/c_0 where v is the velocity of the particle, then in a time t the particle will travel a distance AB $= \beta c_0 t$ and the light will travel a distance AC = (c_0/n).   From this geometry we obtain

$$\cos\theta_c = 1/n\beta \qquad\qquad\text{(eqn 2.2)}$$

which is known as the Cerenkov relation, where θ_c is the direction of emission of the Cerenkov radiation.

Figure 2.2 β vs Electron Energy.

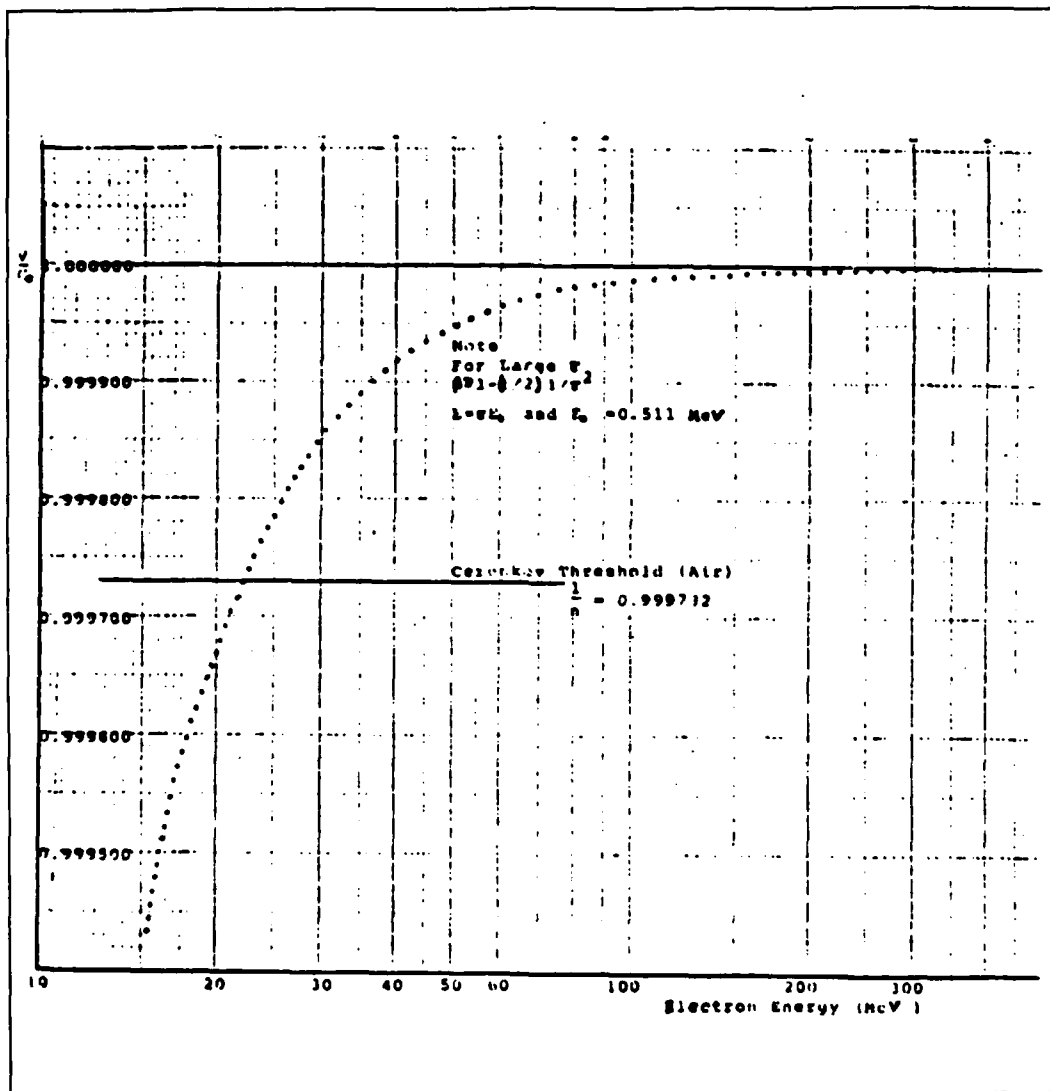It is seen that; for a medium of given refractive index, n, there is a threshold velocity β min = 1/n, below which no radiation takes place. Figure 2.2 shows a relationship between β (i.e., v/c_e) and electron energy in Mev. Note that, in the case of air, 1/n = 0.999732, to achieve Cerenkov radition the electron energy needs to be greater then 22 Mev. At this critical energy the direction of radiation of coincides with that of the particle(i.e., along the path of the particle).

The above discussion applies to the case where the path of the charge bunch is infinite. For a finite path, the phasing condition between the charge and the radiation is relaxed so that the sharp Cerenkov radition peak is broadened over a range of angles. The resulting radiation is given by

$$W(\nu, \hat{n}) = \nu_o{}^2 Q R^2 \qquad \text{(eqn 2.3)}$$

for a beam of periodic bunches of fundamental frequency , and by

$$E(\nu, \hat{n}) d\nu = Q R^2 d\nu \qquad \text{(eqn 2.4)}$$

for a single charge bunch. Here W is radiated power in watts/sr at the integral harmonic frequency

$$\nu = j\nu_o \qquad \text{(eqn 2.5)}$$

and E is the energy radiated per unit solid angle per unit frequency range(Joules/sr/Hz). In either case, Q is the constant

$$Q = \frac{\mu c q^2}{8\pi^2} \qquad \text{(eqn 2.6)}$$

13

where μ is the magnetic susuptibility of the medium, c is the velocity of the radiation in the medium, and q is the charge in a single bunch. The radiation function R is the same in both cases

$$R = kL \sin\theta \, I(u) \, F(k) \qquad \text{(eqn 2.7)}$$

where

$$I(u) = (\sin u)/u \qquad \text{(eqn 2.8)}$$

where k is wave vector, L is the finite propagating distance of the electrons, F(k) is a dimensionless form factor, i.e., the Fourier transform of the charge bunch is qF(k), and the radiation parameter u is given by $u = kL(\cos\theta_c - \cos\theta)/2$. In the *forward* direction, the radiation function (and thus the radiation)is dominated by the diffraction function I(u), which has a maximum at u = 0 and adjacent zeroes at $(+)\pi$ and $(-)\pi$. In the variable θ , the maximum corresponds to $\theta = \theta_c$ and the zeroes correspond to

$$\cos\theta_1 = (n\beta)^{-1} + \eta^{-1} \quad (u = -\pi) \qquad \text{(eqn 2.9)}$$

$$\cos\theta_2 = (n\beta)^{-1} - \eta^{-1} \quad (u = +\pi) \qquad \text{(eqn 2.10)}$$

respectively, where $\eta = L/\lambda$ and λ is the wavelength in the medium of the rediation.

For a infinite path, $\theta_1 = \theta_2$ and the radiation peak is very sharp. For a finite path, θ_2 and θ_1 differ more and more as the path becomes shorter. The onset of radiation is defined as the condition when θ_2 just enters the physical range ($\cos\theta_2 = 1$).

14

This situation may arise through various combinations of index of refraction, beam energy and beam length.

The index of refraction of air is close to 1 and its variation with temperature or pressure is very small so that the effects of changes in the constant Q are inconsequential. Otherwise the index of refraction n enters the formalism only through the parameter u. Here, however the effects may not be completely neglible since the radiation patterns and the onset of radiation are sensitive to u.

B.   INDEX OF REFRACTION FOR THE ATMOSPHERE

To obtain a reasonable understanding of the index of refraction for the atmosphere, we must consider some basic physical principles. These considerations are necessary if one is to have an appreciation for the relative effects of pressure, temperature and water vapor. *From previous* discussion, the index of refraction was determined by the dielectric constant, ε, ($n = \sqrt{\varepsilon}$).

The atmosphere is a gas, and Debye derived an expression that relates the dielectric constant, ε, of a gas to its basic properites. The equation is

$$\frac{\varepsilon-1}{\varepsilon+2} = \frac{4\pi}{3} \frac{\overset{\circ}{A}}{M} \rho[\alpha + \frac{1}{3} \frac{\mu^2}{KT} (\frac{1}{1+i\omega\tau})] \qquad \text{(eqn 2.11)}$$

amount of material   polarizability   permanent dipole contribution

The physical meaning of each term is indicated in the equation. The symbols are as follows, $\overset{\circ}{A}$ = Avagadros number, ρ = density, K = Boltzmans constant, M = molecular weight, μ = permanent electric dipole moment, τ = the relaxation time required for external field-induced orientation of the molecules to return to a random distribution after the field

15

is removed, $\omega = 2\pi f$ where f is the frequency of the external field.

One concludes from Debye's analysis that for external fields with freqencies less than 100 GHz/s, $\omega\tau << 1$, with the result that eqn 2.11 is written as

$$\frac{\varepsilon-1}{\varepsilon+2} = \frac{4\pi\dot{A}\rho}{3M} [\alpha' + \frac{\mu^2}{3KT}] \qquad \text{(eqn 2.12)}$$

This expression contains two of the influences of an externally impressed field decribed previously. The poiarizability is due to the distortion of the molecules by the impressed field. It is noted that both non-polar and polar molecules experience distortion. The permanent dipole contribution is due to the orientation effect on the polar molecules only.

Since $n = \sqrt{\varepsilon}$ and since $n \neq 1$ we approximate

$$\frac{\varepsilon-1}{\varepsilon+2} = \frac{n^2-1}{n^2+2} \approx \frac{2(n-1)}{3} \qquad \text{(eqn 2.13)}$$

Using the above expression we can write the contributions to n-1 from non-polar (dry) and polar (H O) gases. We also use the equation of state $\rho = P/RT$.

$$\text{(eqn 2.14)}$$

$$(n-1)_{dry} = 2\pi \frac{\dot{A}}{M_d R} \frac{P_d}{T} \alpha_d$$

$$(n-1)_{H_2O} = 2\pi \frac{\dot{A}}{M_\omega R} \frac{e}{T} [\alpha_w + \frac{1}{3}\frac{\mu^2_\omega}{KT}] \qquad \text{(eqn 2.15)}$$

16

It is noted that e is the pressure associated with the water vapor and p_d is the pressure associated with dry air. The total pressure, p , is their sum ($p = p_d + e$). When we add the contributions due to water vapor (polar) and dry air (non-polar) we get the index of refraction of moist air:

$$(n-1) = C_1 \frac{1}{M_d} \frac{P-e}{T} \alpha_d + C_1 \frac{1}{M_\omega} \frac{e}{T} (\alpha_w + C_2 \frac{1}{T}) \qquad \text{(eqn 2.16)}$$

Where $C_2 = \mu\dot{\omega}^2/3K$ and $C_1 = 2\pi\mathring{A}/R$. Note that all parameters in Eqn (2.8) with the exception of p,T, and e can be treated as constants. (M_d and α_d are values averaged over the molecules of the atmosphere.)

If we combine the terms and assign values to the constants we obtain

$$(n-1) = (77.6 \frac{P}{T} - 5.6 \frac{e}{T} + 3.75 \times 10^5 \frac{e}{T^2}) \times 10^{-6} \qquad \text{(eqn 2.17)}$$

where p and e are in millibars and T is in degrees Kelvin. It is very convenient at this point to introduce a new parameter N which is the " Refractivity ",

$$N = (n-1) \times 10 \qquad \text{(eqn 2.18)}$$

From the Ref.(3), this equation becomes

$$N = \frac{288p}{760} \frac{1}{(1+0.003661t)} + \frac{6.7e}{(1+0.003661t)^2} \qquad \text{(eqn 2.19)}$$

Where p and e are in millibars and t is in degrees Celsius (°C), n is the refractive index, defined as the ratio of velocity of propagation of the electromagnetic wave in a

17

vacuum to that in air. Since electromagnetic waves travel
slightly more slowly in air than in a vacuum, the refractive
index is always slightly greater than unity. At the earth's
surface the numerical value of the refractive index is
usually between 1.000250 and 1.000400. The value N is thus
between 250 and 400. Refractivity can be expressed as a
function of the atmosphere pressure, temperature, and
humidity by the Equation (2.19).

Figure 2.3   Refractivity Profiles in the Standard Atmosphere
from Ref. 2.

In Figure (2.3), refractivity is shown as a function of
altitude for surface refractivities of 240 and 400 N-units
for standard atmosphere conditions. In the calculations to
plot curves, layer thicknesses of constant refractivity of
50 meters were taken from the ground level to an altitude of

18

30 Km. The region above that was considered to consist of
unity refractive index [Ref. 2].

III. CALCULATION OF REFRACTION INDEX IN THE ATMOSPHERE

A. TEMPERATURE IN THE ATMOSPHERE

The temperaturer of the surface air is well known at many places and various heights, from sea level up to about 6 kilometers. But the temperature records obtained by the aids of kites and balloons, both manned and free, show that the mountain air temperatures generally differ materially from the temperature of the free air at the same height and latitude.

The average temperature of the surface decreases approximately at the rate of 1°C per each 180 meters, 200 meters, and 250 meters increase of height on mountains, hills, and plateaus, respectively. In the free atmosphere, however, the result is quite different.Here the decrease of temperature with increase of altitude, except at very great heights is, roughly, the same at most parts of the world. Figure(3.1) from [Ref.13] shows at thetemperature decreases linearly between sea level and an altitude of 10 Km.

B. PRESSURE IN THE ATMOSPHERE

Atmospheric pressure (air pressure) is the force of hydrostatic pressure of air acting on a unit area. In immobile air it is equal to the buoyancy of air and is balanced at every point by the weight of a vertical column of air of unit cross section lying over the level under consideration.
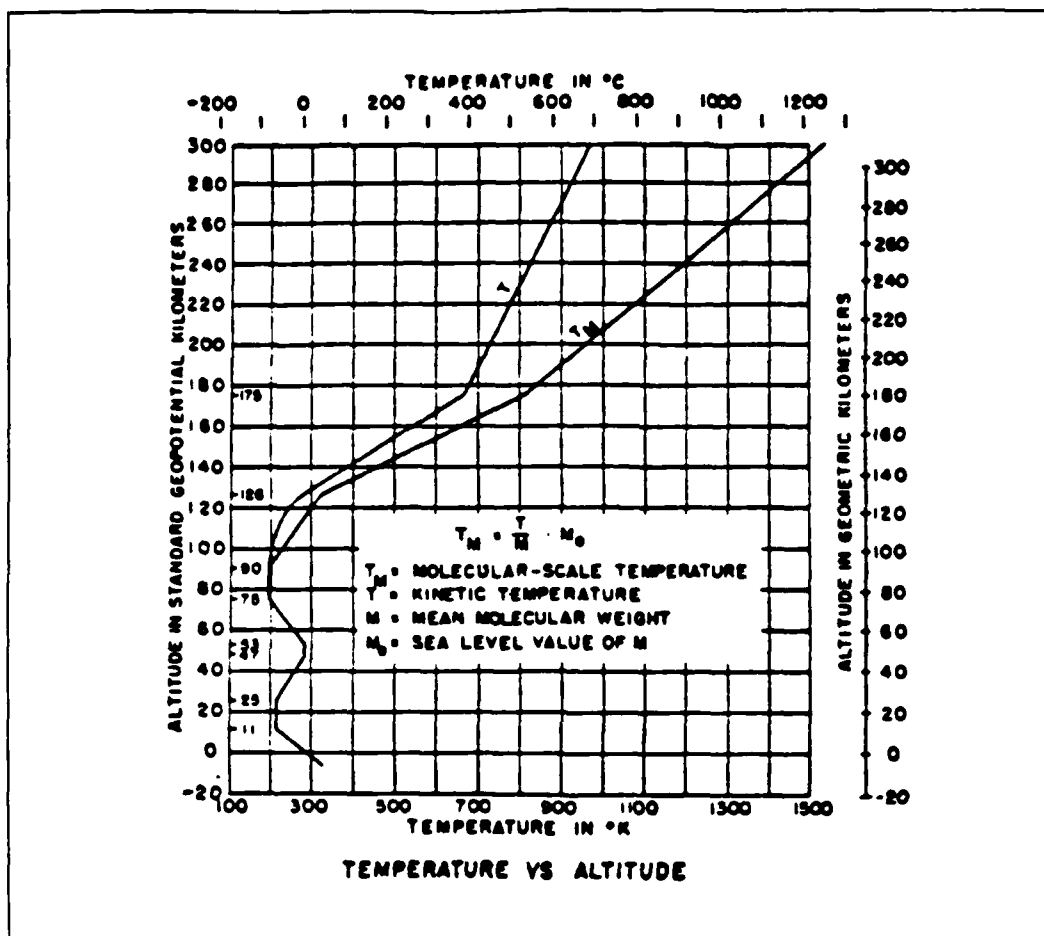
Figure 3.1   Temperature Profiles in the Atmosphere
from Ref.13.

In practice, pressure is usually measured in terms of
the height of a column of mercury in a barometer, expressed
in millimeters (mmHg). But the height of the mercury
column in a barometer, as is well known, depends not only on
pressure but also on the temperature of the mercury, as well
as   on   the   acceleration   of   gravity   at   the   point   of
observation, which varies with elevation above sea level and
latitude. The reading of a mercury barometer must therefore
be reduced to a standard temperature (usually 0° C), and a
standard altitude and latitude. Figure (3.2) from [Ref.13]

shows the pressure decreases almost linearly between sea
level and an altitude of 40 Km.

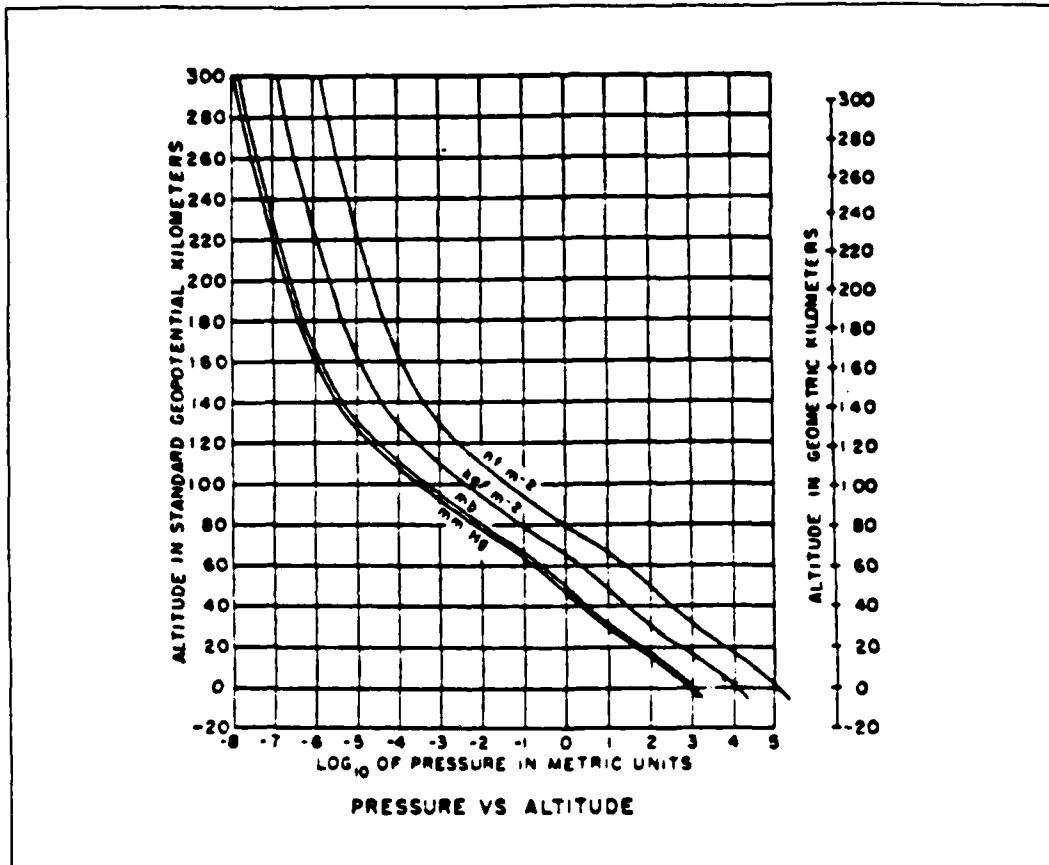Figure 3.2   Pressure Profiles in the Atmosphere
from Ref.13.

C. WATER VAPOR IN THE ATMOSPHERE

Water vapor enters the atmosphere because of the
evaporation of water from the earth's surface and spreads
through the atmosphere by mixing. At the same time the
maximum content of water vapor is restricted by its
saturation pressure; condensation of the vapor takes place
when this point is reached.

The processes of evaporation and condensation are accompanied by the absorption or generation of heat, which is reflected in the thermal regime of the corresponding layers of the atmosphere. Water vapor also plays a large part in the processes of absorption and emission of radiation. All this explains the tremendous role of water vapor in all phenomena in the atmosphere. The mean vapor pressure e depends exponentially on the height above sea level.

$$e = e_o \ 10^{-\frac{z}{\beta}}$$
(eqn 3.1)

Here e and e_o are the mean vapor pressure at height z and at the surface respectively. The coefficient β is found from observational data. For the lower atmosphere, β is about 5000m. From this it follows that e decreases by a factor of 10 at a height of 5Km, a factor of 2 at 1.5 - 2 Km, etc, i.e., The vertical decrease of the vapor pressure is much faster than that of the overall pressure of the atmosphere. The concentration of water vapor also decreases (exponentially) with altitude. Thus the vapor content falls off very rapidly with altitude and becomes negligible when a level of about 8 - 10 Km is reached; at great altitudes the air is, as a rule, very dry(Figure 3.3).

D. CALCULATION DATA

Table I and II show the parameter for the US standard atmosphere [Ref.3] and the German atmosphere [Ref.4]. Using these data in equation 2.19, the microwave index of refraction can be calculated [Ref.5] as shown in Table III and IV. These results are then used to assess the changes in microwave Cerenkov radiation resulting from propagation of an electron beam in the atmosphere.
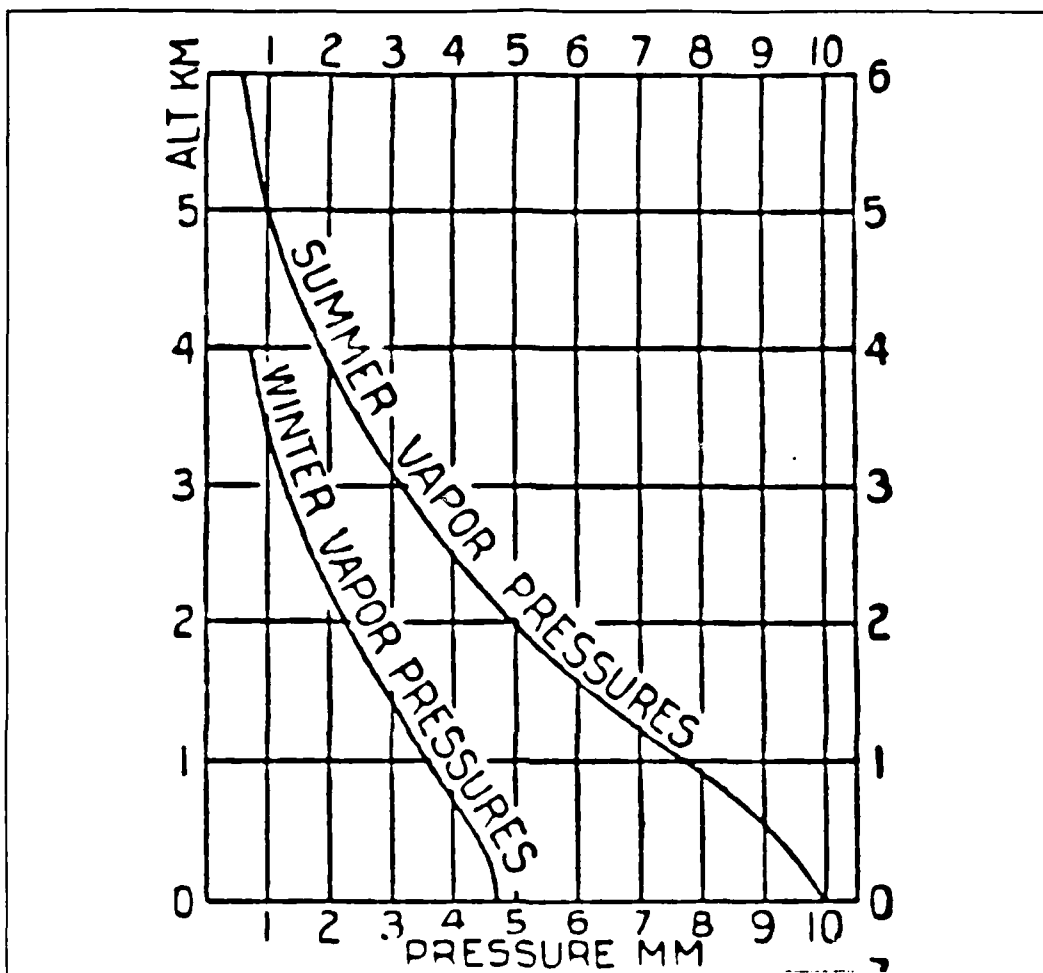
23

Figure 3.3   Water Vapor Profiles in the Atmosphere
from Ref.4.

24

TABLE I
U.S. STANDARD ATMOSPHERE

Alt. (Km)	Temp. (°C)	Pressure(mmHg)		
		air	vapor	saturation
0	15	760.000	5.683	12.785
1	8.5	674.160	3.987	8.3202
2	2	596.337	2.713	5.292
3	-4.49	525.978	1.428	3.283
4	-10.98	462.512	0.941	1.983
5	-17.47	405.414	0.568	1.164
10	-49.9	198.78	0.014	0.057
0	37	760.000	47.067(extreme)	

TABLE II
GERMAN ATMOSPHERE (MEAN 1900-1912)

Alt. (Km)	Temp. (°C)	Pressure(mmHg)		
		air	vapor	saturation
0	15	762.950	7.5750	12.785
1	8.5	675.680	5.685	8.3202
2	2	597.340	3.620	5.292
3	-4.49	526.910	2.210	3.283
4	-10.98	463.570	1.295	1.983
5	-17.47	406.630	0.530	1.164
10	-49.9	199.480		0.057

TABLE III
INDEX OF REFRACTION IN U.S. STANDARD ATMOSPHERE

Alt. (Km)	Temp. (°C)	Index(n) dry air	vapor	saturation
0	15	1.000273	1.000307	1.000351
1	8.5	1.000248	1.000273	1.000301
2	2	1.000224	1.000242	1.000261
3	-4.49	1.000203	1.000213	1.000227
4	-10.98	1.000183	1.000190	1.000199
5	-17.47	1.000164	1.000169	1.000194
10	-49.9	1.000092	1.000092	1.000093
0	37	1.000498(extreme)		

TABLE IV
INDEX OF REFRACTION OF GERMAN ATMOSPHERE

Alt. (Km)	Temp. (°C)	Index(n) dry air	vapor	saturation
0	15	1.000274	1.000320	1.000351
1	8.5	1.000248	1.000284	1.000301
2	2	1.000225	1.000249	1.000261
3	-4.49	1.000203	1.000218	1.000227
4	-10.98	1.000183	1.000192	1.000199
5	-17.47	1.000164	1.000169	1.000194
10	-49.9	1.000092		1.000096

IV. EFFECTS OF CHANGES INDEX OF REFRACTION ON CERENKOV RADIATION

A. EMISSION THRESHOLD FOR COHERENT CERENKOV

We define the onset of the emission of Cerenkov radiation to be the situation when $\theta_\perp$ begins to enter the physical range [Ref.6]. Then setting $\theta_\perp = 0$ in eqn. 2.10 gives

$$n\beta = \eta \, (\eta+1)^{-1} \qquad\qquad \text{(eqn 4.1)}$$

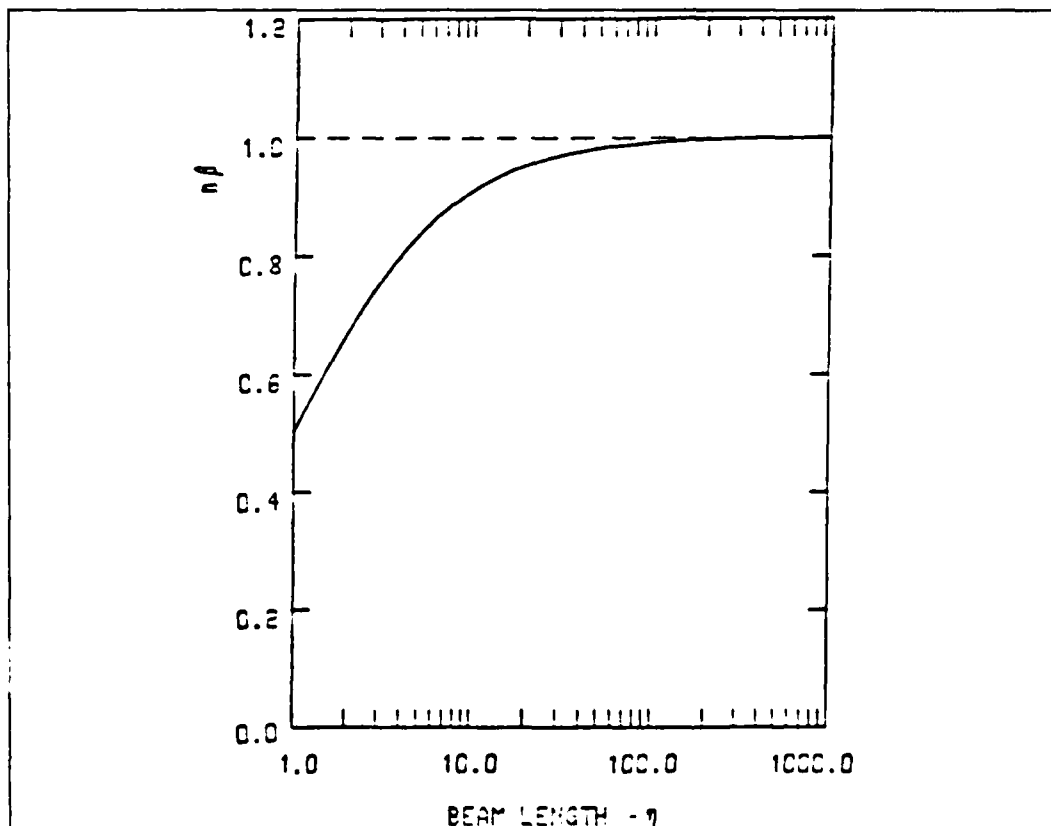A plot of eqn.4.1 is shown in Figure 4.1.

Figure 4.1   Threshold of Emission.

As beam length increases, the product $n\beta$ first rises rapidly and then asymptotically approaches the value unity. Any value of $n\beta$ above the curve gives Cerenkov radiation with a peak position dependent on the beam length. That is, for values of $n\beta > 1$, the Cerenkov angle θ_c is in the physical range. For values of $n\beta$ between the curve and unity, θ_c is non physical but radiation with a well defined peak is still produced.

Using the usual relation between β and γ, Equation 4.1 can be put in terms of γ_t, the value of γ necessary for the onset of Cerenkov Radiation.

$$\gamma_t(n) = \left[1 - \frac{1}{n^2(1+n^{-1})^2}\right]^{-1/2} \qquad \text{(eqn 4.2)}$$

This gives the required energy $E_t = \gamma_t E$ for the onset of emission in terms of the index of refraction n and the beam length.

Limiting values of equation 4.2 can be obtained for very long and very short beam lengths. For infinite beam length,

$$\gamma_t(n \to \infty) = \left[1 - \frac{1}{n^2}\right]^{1/2} \qquad \text{(eqn 4.3)}$$

which decreases and approaches the value of 1 as n increases.

Table III and IV show that the entire range of index of refraction is between the 10 Km value n = 1.000092 and the surface water saturated value of n = 1.000500 for extreme condtions. In the following, the effects of variation of the index between these limits on the size and position of the first radiation lobe, the threshold electron energy for emission, and the radiation patterns, are assesed.
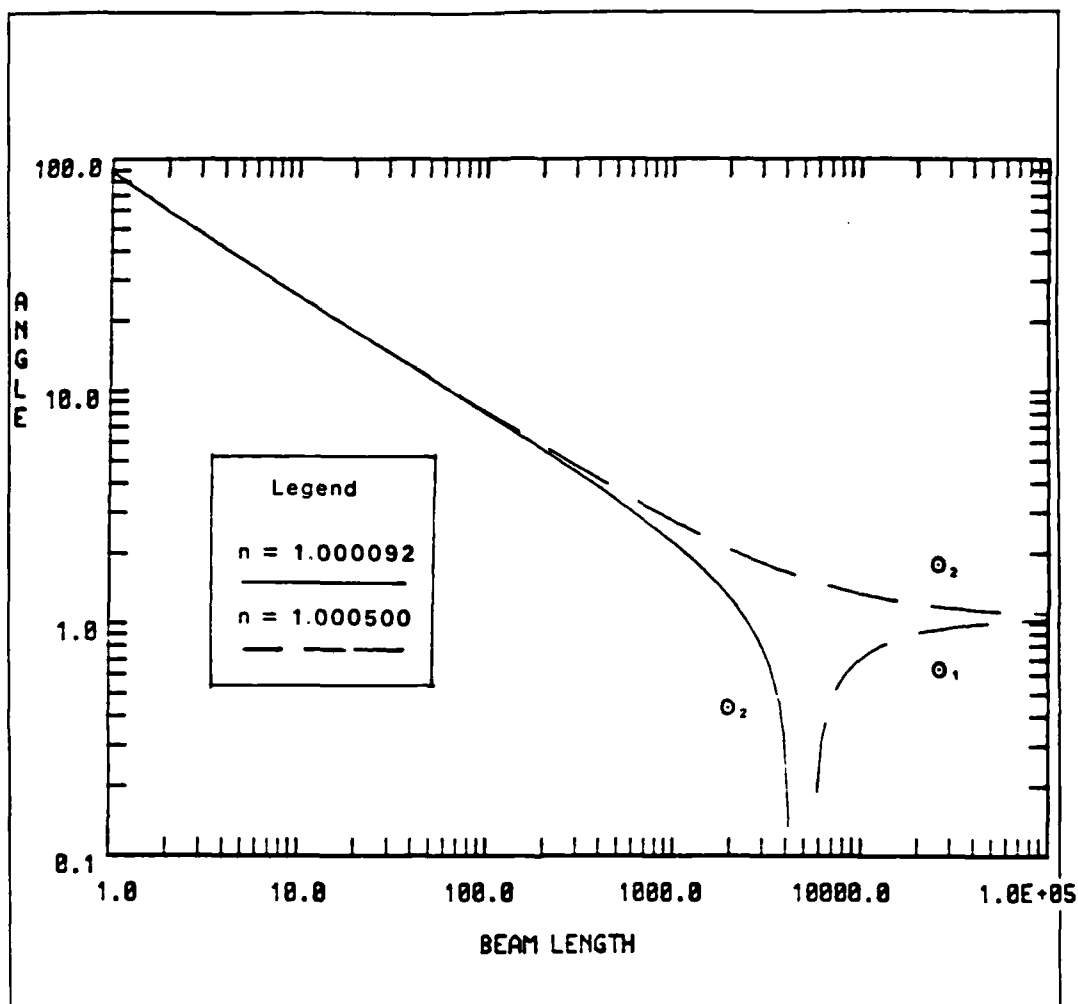
Figure 4.2   First Diffraction Lobe Limits
for 20 MeV Electron Bunches.

The bounds θ_u and θ_l for the first diffraction lobe are given by eqn 2.9 and eqn 2.10 with the principal maximum lying between. Figure 4.2, 4.3, 4.4, show the first diffraction lobe angular limits θ_u and θ_l as a function of beam length parameter   for 20 MeV, 100 MeV, and 1000 MeV, electron bunches.   In   these   figures,   the   solid   line represents calculations for the minium index of refraction
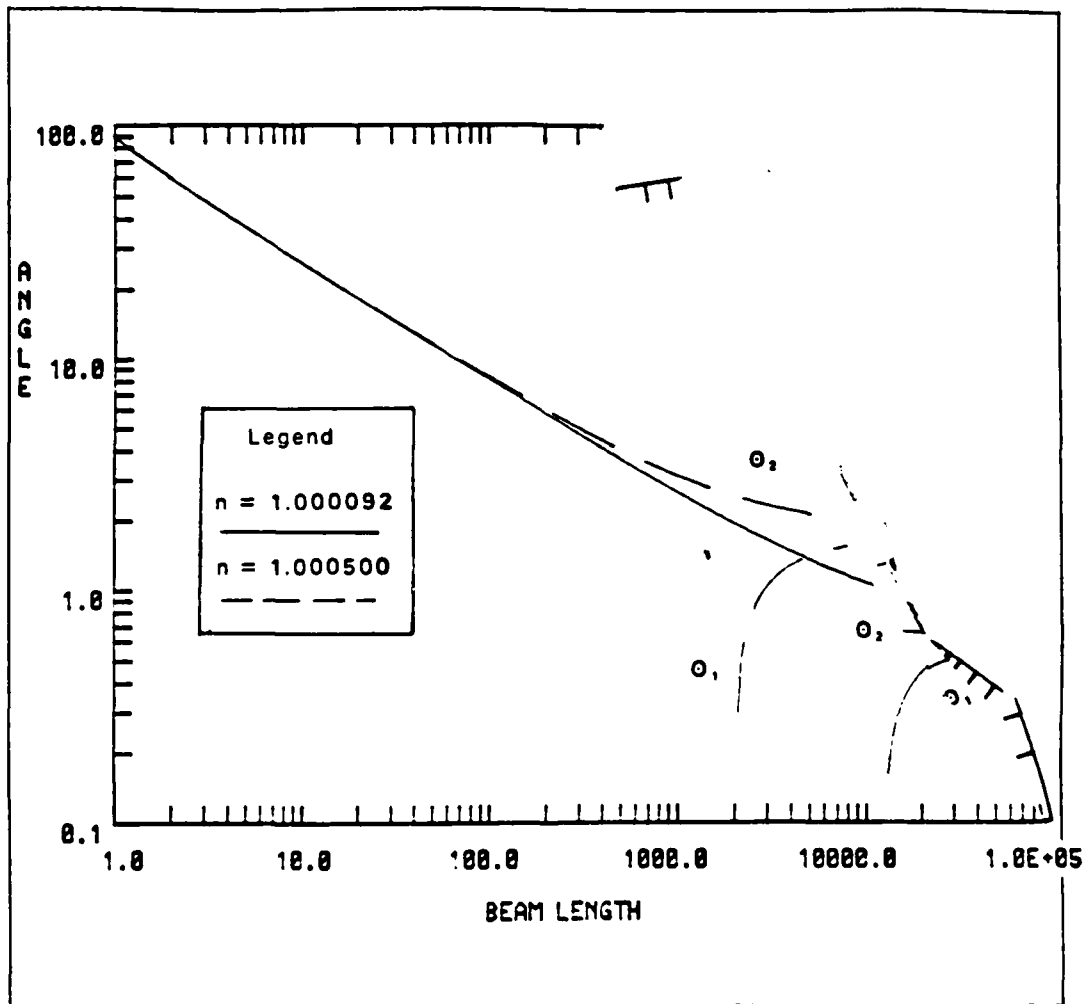
29

Figure 4.3   First Diffraction Lobe Limits
for 100 MeV Electron Bunches.

in the atmosphere and curve of large dashes marks the
calculations for the maximum index of refraction in the
atmosphere.

In figure 4.3, θ_u and θ_l are given by the upper and lower
curve of each pair. In both cases, θ_u is large for short
beam lengths, and θ_l is nonphysical. As the beam length
increases, θ_u falls and θ_l becomes physical and increases.
Then in the limit of very long path, both angles converge
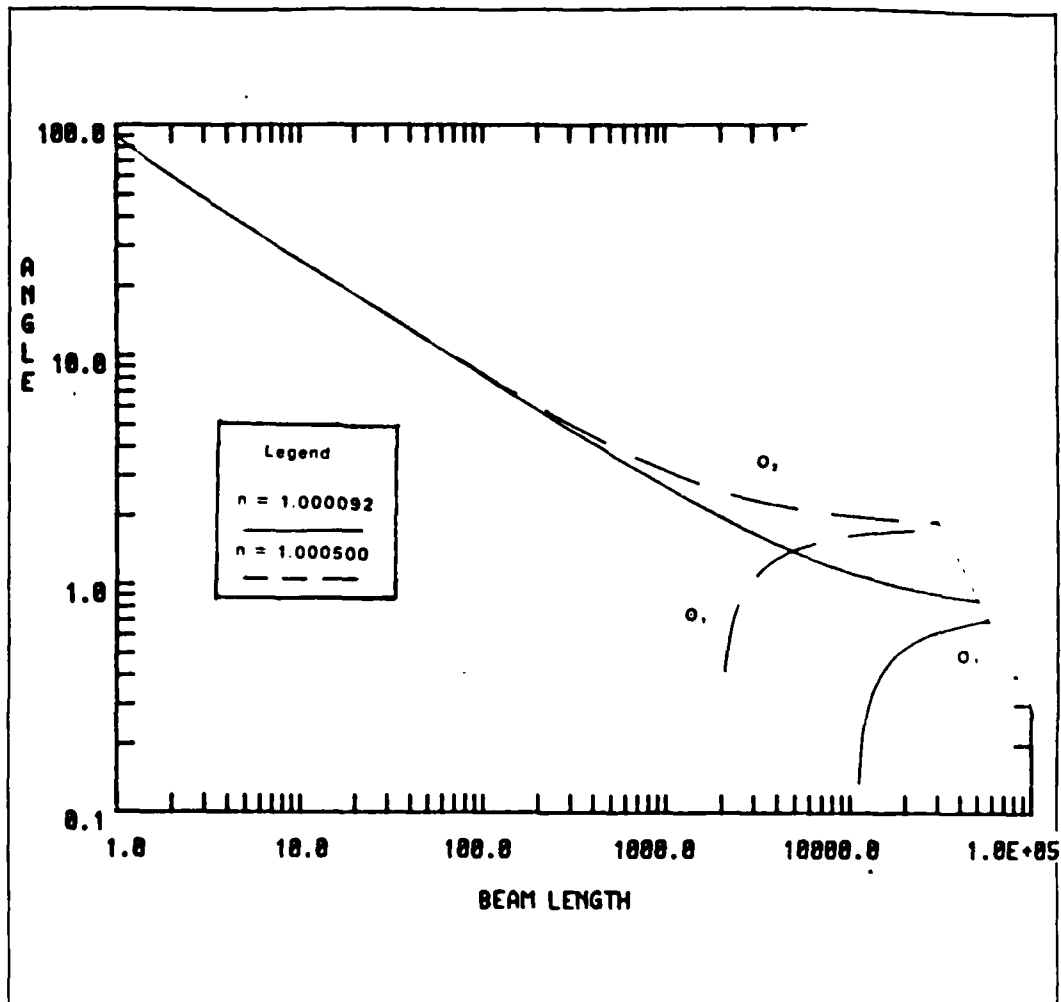to the value θ_c which is different for air of differing

30

Figure 4.4   First Diffraction Lobe Limits
for 1000 MeV Electron Bunches.

index of refraction (θ_c = 1.81° the for upper curve and θ_c =
0.78° for the lower curve).

At an energy of 100 MeV, an electron is already moving
very close to the speed of light as shown in Figure 2.2.
Consquently, increasing the electron energy to higher values
has only a very small effects.   This is shown in Figure 4.4
which differs only slightly from Figure 4.3.   However, at
energies lower than 100 MeV the electron velocity is a much
stronger function of energy and at 20 MeV the electron

31

velocity is significantly smaller than c_o . The effects of this change are shown is Figure 4.2 where the dashed curve (air saturated with vapor) is similar to the dashed curves in Figure 4.3 and 4.4 except that the limiting value of θ_c is much smaller. However, The behavior of the curves for the 10 Km index of refraction (n = 1.000092) are different. For these values of the index and electron energy, $n\beta < 1$ so that θ_c is non physical and θ_i does not exist for any value of the beam length. The behavior of θ_λ at short beam length is the same as that for higher energies, but at longer beam lengths θ_λ falls precipitously to zero so that there is no Cerenkov radiation in the limits of very long paths.

The value of $\vdash$ necessary for θ_λ to become physical is given by eqn 4.2, and is calculated for electrons in Figure 4.5. Again, the solid curve is for the upper atmosphere value of the index and the dashed curve is for the saturated value. At short beam lengths the curves are identical, but at longer beam lengths the electrons require a higher velocity (through an increase in energy) in order for θ_λ to become physical.
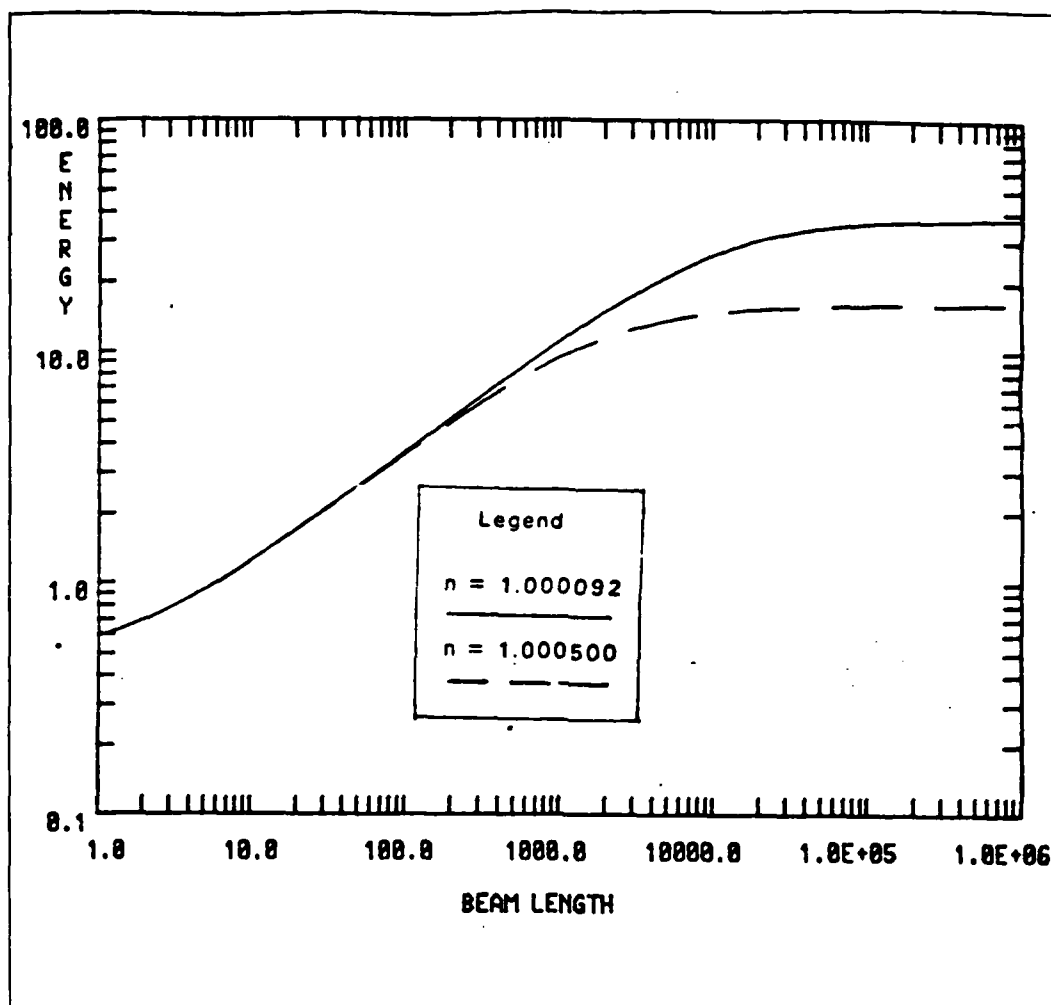
Figure 4.5   Threshold Electron Bunch Energies.

The interpretation of the curves in Figure 4.5 is as follows; If a given physical situation is represented as a point with coordinates E and η on the graph, when that point lies below the curve, Cerenkov radiation is not produced. Above the curve, but below the threshold energy for infinite path, is the transition region in which the radiation peak continuously increases in size but changes position only slightly.   Above the threshold energy for infinite path, Cerenkov radiation is always produced, with an associated narrowing of the first lobe as the path increases.

33

The indices of refraction are 1.000092 for upper solid line and 1.000500 for the lower large dashed line. Until a beam length of about $\eta = 100$, is reached, the minimum index of refraction and maximum index of refraction do not affect the threshold energy in the atmosphere. After that value, the minimum index of refraction slightly more affects to the energy.

B. RADIATION PATTERNS

Figure 4.6 through 4.12 show the effects of changes in the index of refraction on the radiation function R. These are all calculated for parameters of the NPS Linac: a fundamental frequency of 2.85 GHz and assuming a Gaussion charge distribution within a rigid electron bunch but with variable energy.

The beam length parameter $\eta = L/\lambda$ enters into R directly and through u. Using the frequency of 2.85 GHz leads to a wavelength in the medium (air) of 10.49 cm for the fundamental. All of the beam lengths(η) are calculated using this value of wavelength.

Figure 4.6 shows the calculated power W(watts/steradian) radiated from a periodic beam of electron bunches traversing a path (beam length) of 100.0 cm for media of three different values of index; n = 1.000268 n = 1.000092 and n = 1.000500. In this case, all three radiation patterns are identical and show a broadening of the radiation pattern as a result of diffraction due to the small size of the source.

Figure 4.7 is calculated for 100 MeV electrons and a path length of L = 10,490 cm ($\eta = 10$). At this longer path length the radiation peak is narrowed and heightened, and the maximum value occurs at a smaller angle. Differences are readily apparent between the pattern for the different indices. Here, the dotted line represents a nominal sea level dry air value (n = 1.000268) and the dashed and

34

solid line represents the 10 Km and saturated value respectively.

The upper bound of the main lobe is given by eqn 2.9 . Inspection of this relation shows that θ_λ as well as θ_c increases with increasing index of refraction. This is shown clearly in Figure 4.7 where the first zero of the radiated power is least for the lowest index and then increases with increasing index. The calculated values for θ_λ are 2.66°, 2.87°, and 3.12° corresponding to the respective values of 1.000092, 1.000268, and 1.000500 for the index of refraction. As θ_λ increases the position of the radiation peak also increases and is correspondingly heightened by the Sin 0 factor in the radiation function R .

Large changes in the radiated power occur when the parameters change so as to pass the emission threshold boundary delineated in Figure 4.2, 4.3 and 4.4. At a beam length of L =10.494 x 10 cm (η = 10) the calculated threshold value for electron boundes is 21.676 MeV for nominal sea level dry air, n = 1.000268. Small departures from these values of the parameters can allow the threshold to be crossed with dramatic results.

Figure 4.8 is shows the calculated radiated power as a function of angle for electron bunches having a beam length of η = 10 and an energy one percent below the above threshold of 21.676 MeV. The dotted line calculatedusing the nominal sea level value of the index (n = 1.000268) shows sub-Cerenkov radiation in an oscillating spatial pattern but without the large principal radiation lobe. Increasing the index to n = 1.000282 (appropriate for sea level with 2.49 mb water vapor at US standard atmosphere) clearly shows the onset of Cerenkov radiation and the increaseing size of the main lobe. Further increase of the index drives the curve higher and to larger angles as β increases.

Figure 4.9 shows the radiated power as a function of angle for the same beam length and energy but for the extrems saturated water value of the index (n = 1.000500). Here the peak power is 15 x 10 W/sr and it impossible to show the curves from the other indices on the same scale.

Figure 4.10 is plotted to an intermediate scale and does show both the n = 1.000282 and the n = 1.000500 curves although the peak for the latter is far off scale. In Fig. 4.9 and Fig. 4.10, the type of line associated with a particular index of refraction is different (for altitu altitude reasons) from the previous figures. When the radiation parameters are far from the threshold values, changes in the index are less drastic.

Figure 4.11 shows the effect of varying the index of refraction on 100 MeV electron bunches with a beam length of η = 100. For this rather short beam the differences in radiated power are small but readily apperent.

The position and size of the peaks corresponding to the different indices are in the same order as Figure 4.7, 4.8, 4.9 and 4.10 for the same reasons.
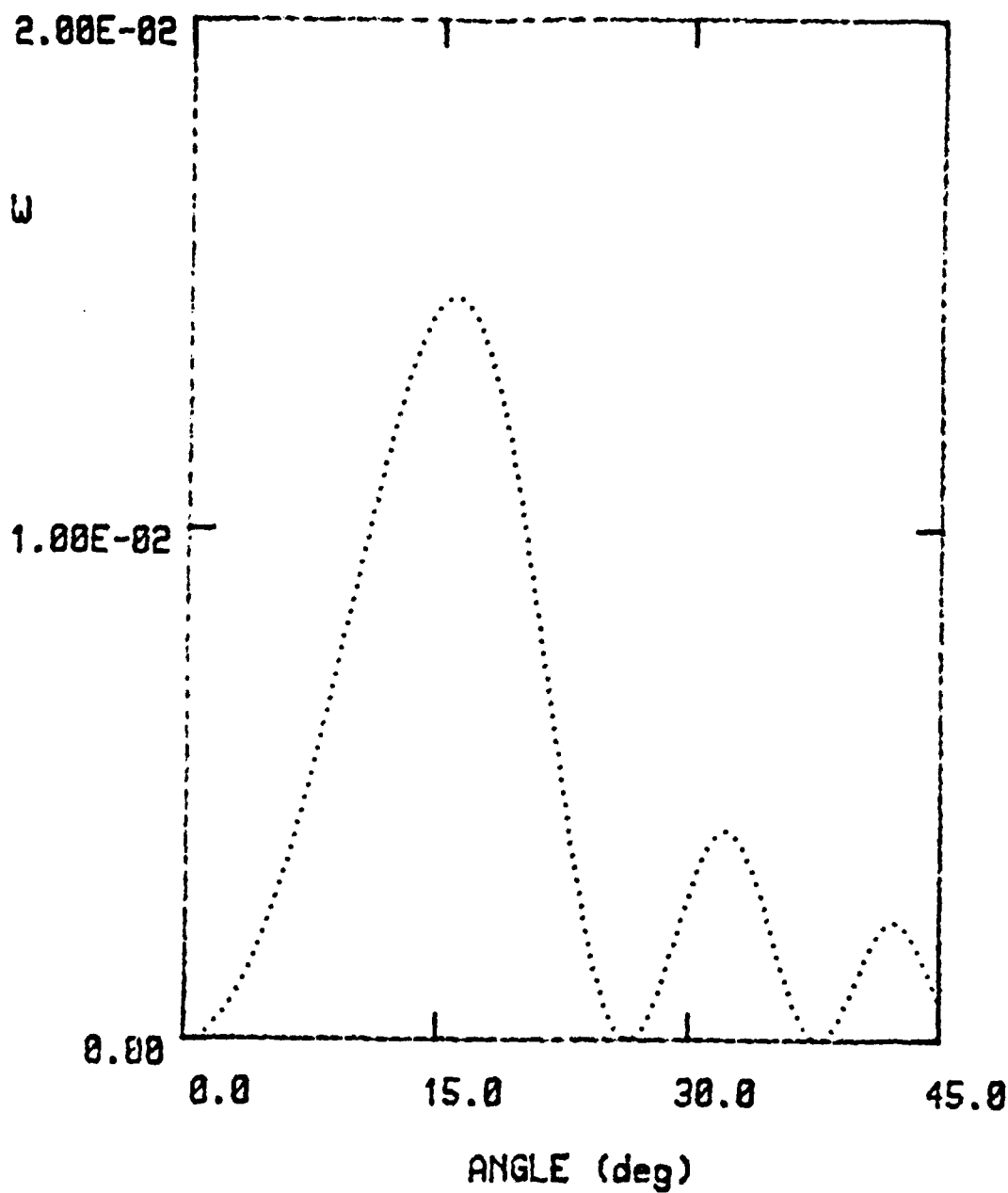
Figure 4.6   Power Radiated vs Angle(1).

Power radiated per unit solid angle (W/sr) as a value of angle for 100 MeV electron bunches and the beam lengths for 100 cm. The function represents three index of refraction n = 1.000092, n = 1.000268, n = 1.000500, i.e; all of which are identical.
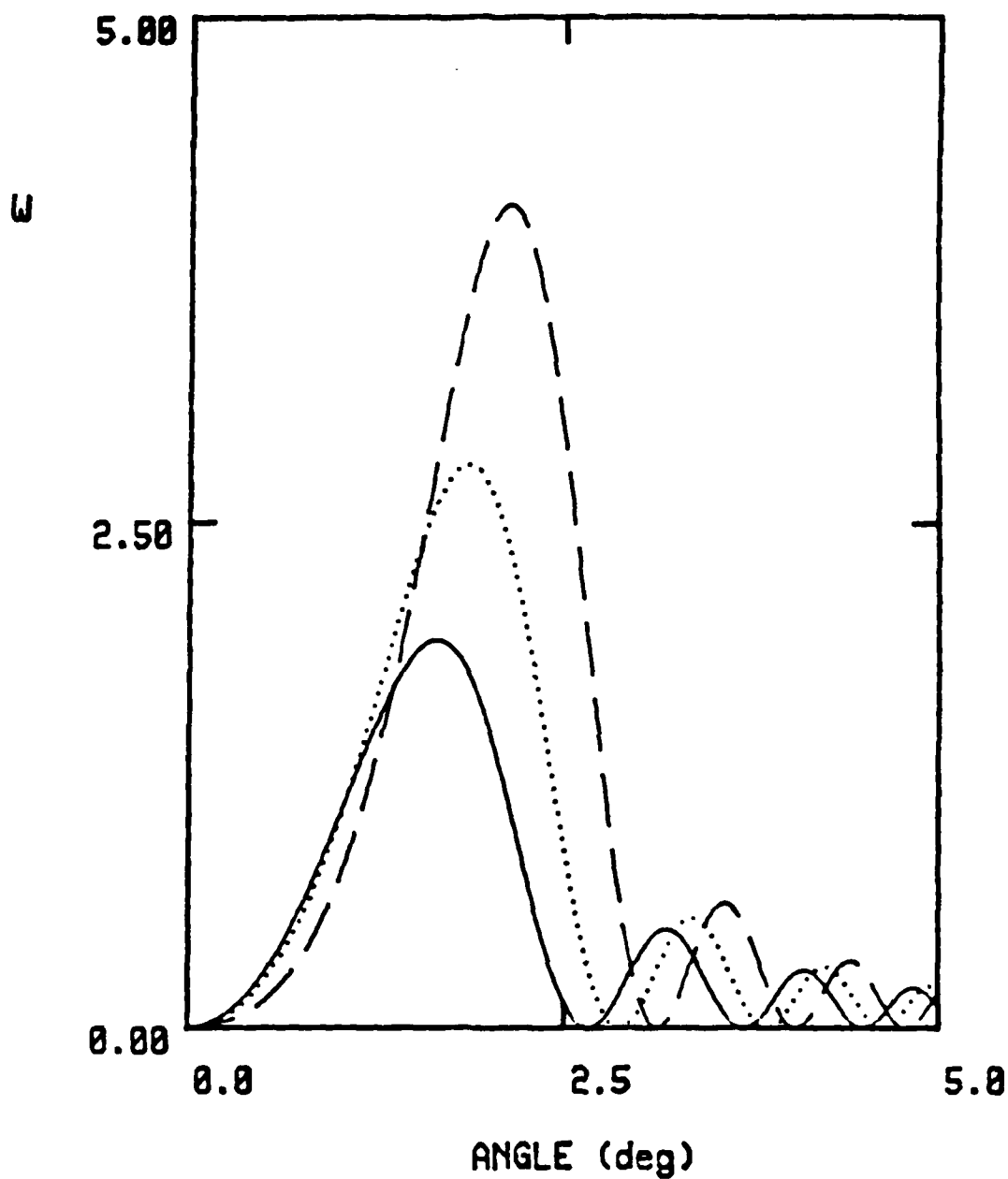
37

Figure 4.7   Power Radiated vs Angle(2).

Power radiated per unit solid angle as a value of angle for
100 Mev electron bunches and a 10490 cm beam length (= 10
), n = 1.000500 for dashed line, n = 1.000268 for dot line,
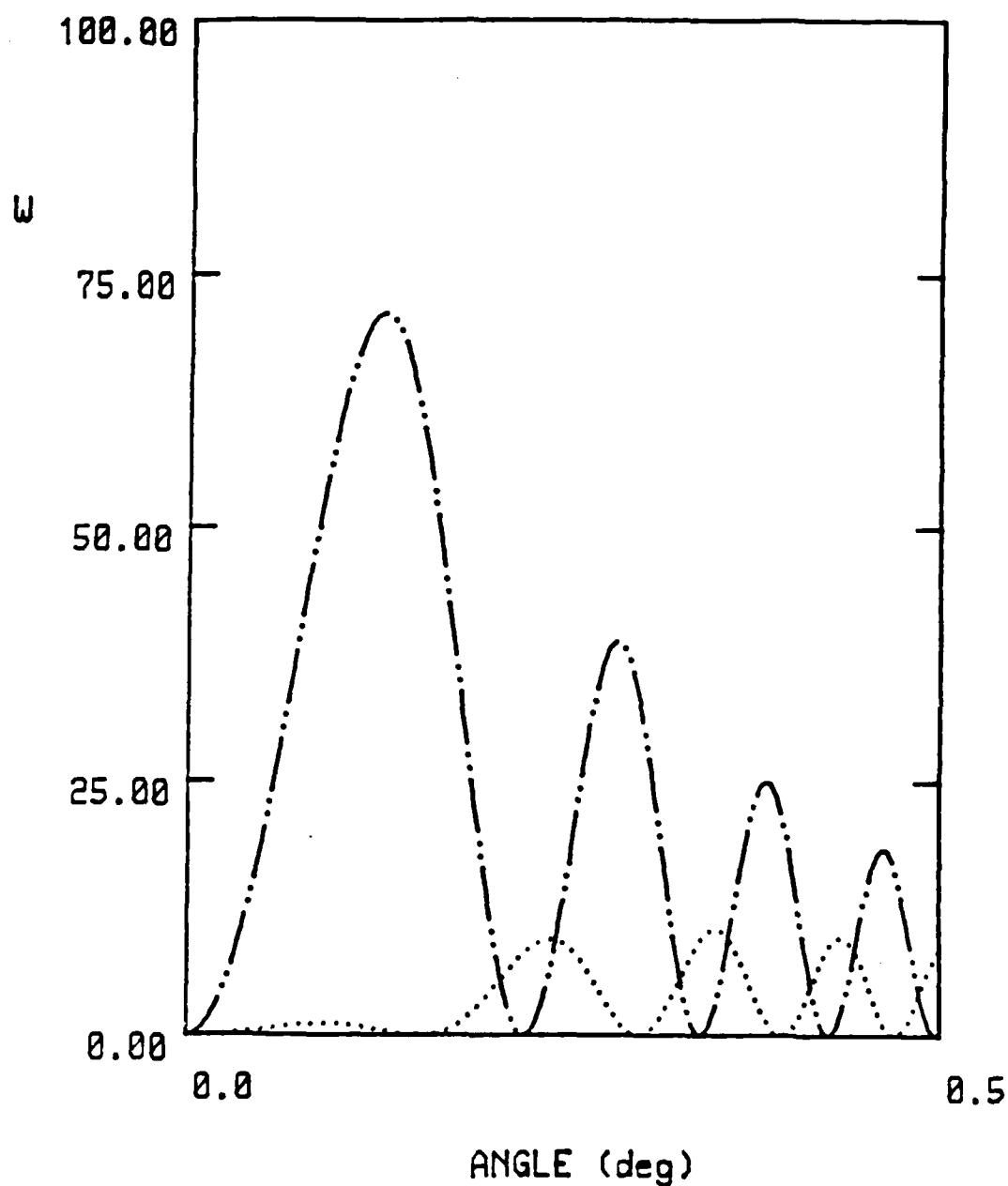n = 1.000092 for solid line.

Figure 4.8   Power Radiated vs Angle(3).

Power radiated per unit solid angle as a value of angle for 21.459 MeV electron bunches and a beam length of 10.494 x 10 cm (= 10), n = 1.000268 for dot line, n = 1.000282 for dashed dot line.   The energy 21.495 MeV is one persent below the threshold for n = 1.000268.
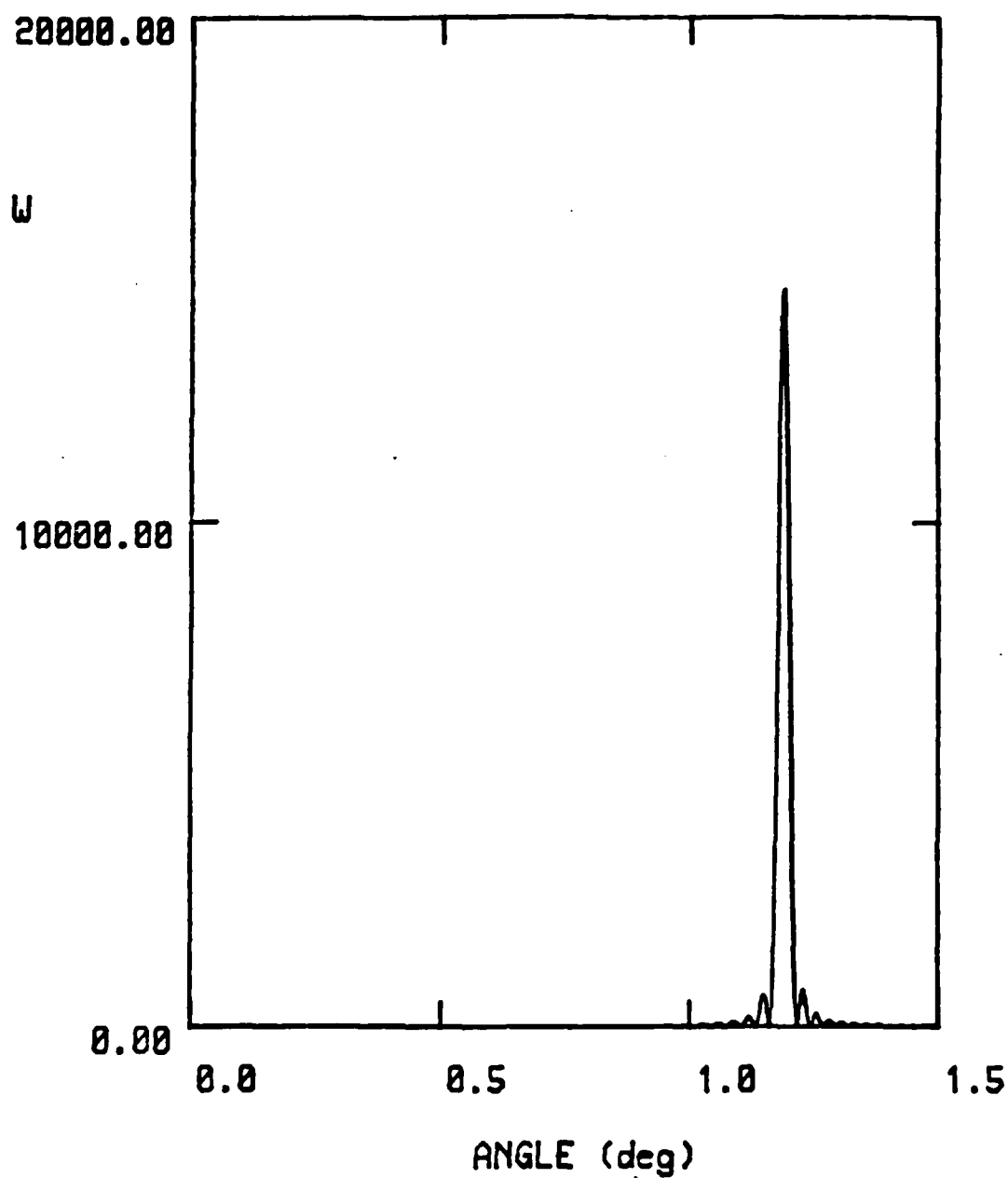
Figure 4.9   Power Radiated vs Angle(4).

Power radiated per unit solid angle as a value of angle for
21.459 MeV, n = 1.000500.   The energy and beam length values
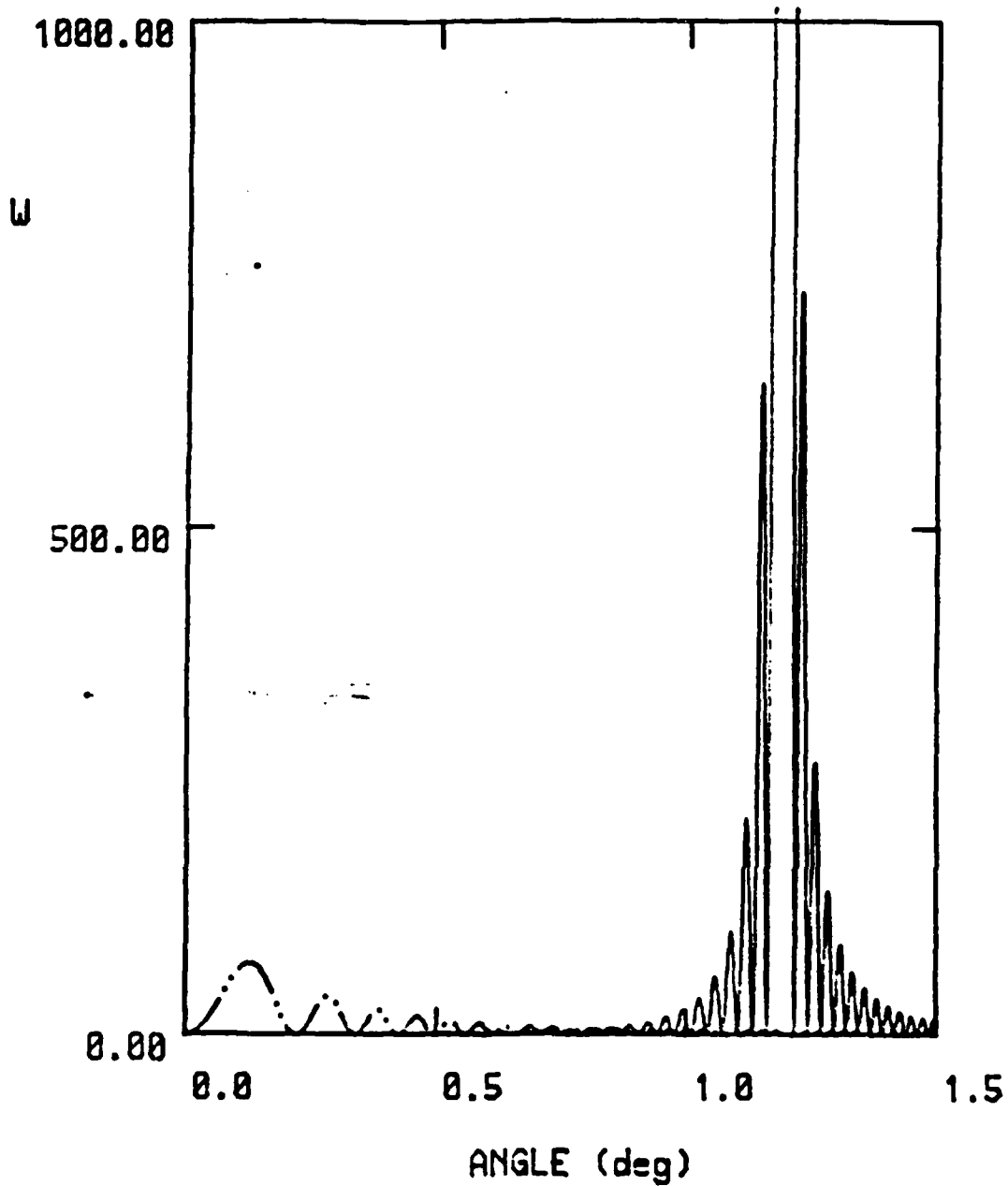are the same as for Fig. 4.8.

Figure 4.10   Power Radiated vs Angle(5).

Power radiated per unit solid angle as a value of the angle
for the same condition of Figure 4.9. This Figure shows the
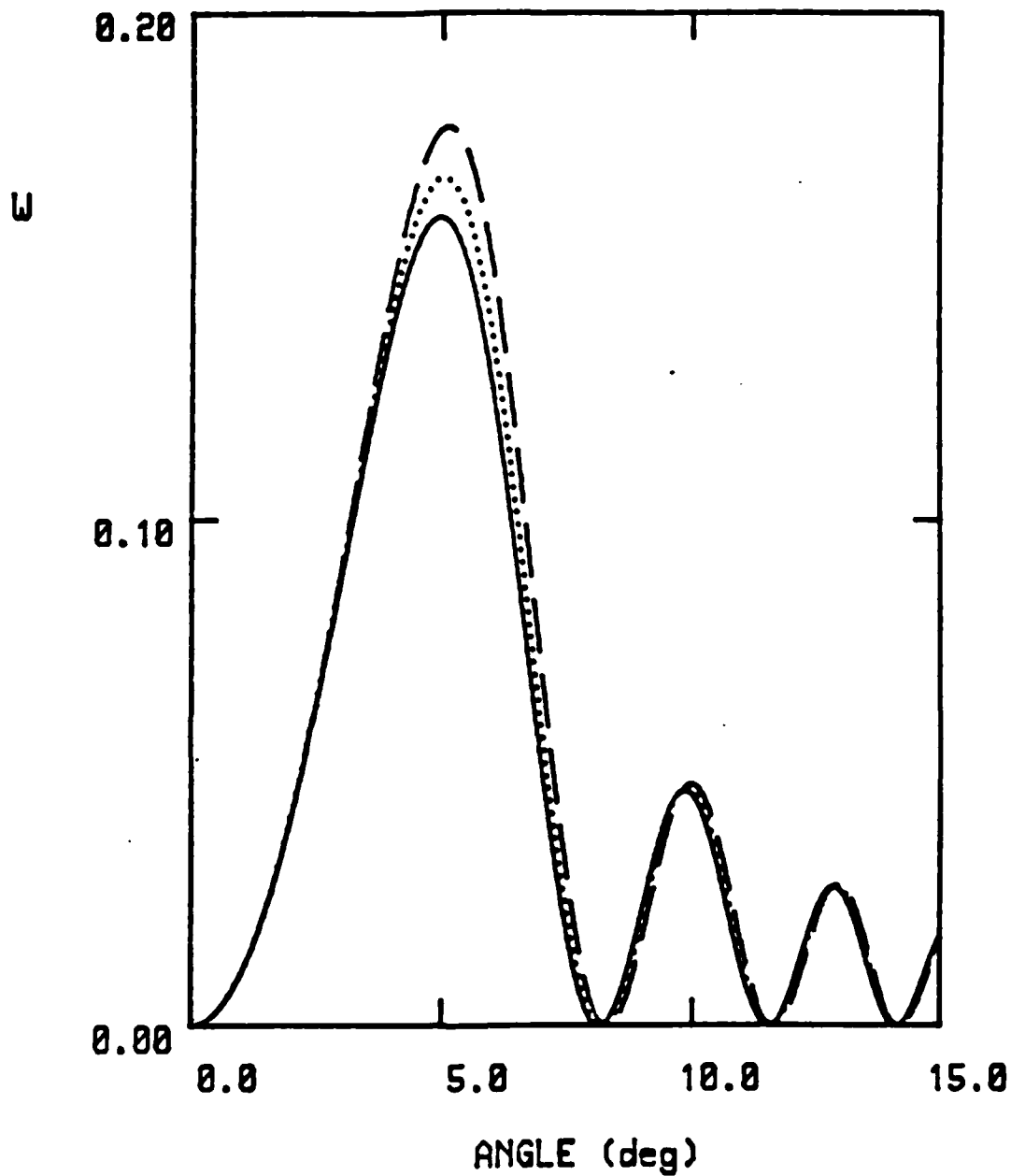radiation pattern for n = 1.000282 (dashed dot line) and n =
1.000500 (solid line).

41

Figure 4.11   Power Radiated v. Angle(6).

Power radiated per unit solid angle as a function of
altitude for L = 1049.0 cm and E = 100 Mev. The nominal dry
sea level for dotted line (n = 1.000273), 10 Km height for
solid line (n = 1.000092), extreme water saturated sea level
for dashed line (n = 1.000500).

V. RESULT AND DISCUSSION

The main points of this paper are to asess, in the GHz frequency region of the electromagnetic spectrum, the effects of height and atmospheric water vapor on the index of refraction, then to determine how this index of refraction affects the radiation pattern and the emission threshold of Cerenkov radiation.

Caculation of the index of refraction for the atmosphere up to 10 Km as shown in Table III and Table IV are new results. The table values vary between 1.000092 and 1.000500. These two values were used in calculating the thresholds, radiation pattern, and angular limits of the radiation pattern.

The principal results of this study are;

1. For high energy electron beams the principal radiation lobe is concentrated in a narrow range about the angle θ_c as the beam length increases. The particular value of θ_c depends on the value of the index of refraction with larger indices giving larger values of θ_c.

2. For low energy beams, the lobe may or may not narrow depending on the value of the index.

3. The threshold energy value for the onset of Cerenkov radiation at long beam lengths is strongly affected by changes in the index of refraction.

For a specific example, using Fig. 4.5, the variation of index of $\Delta n/n = 0.000408$ gives an approximate doubling of the threshold energy.

4. The radiation patterns for long beam lengths are sensitive to changes in the index of refraction. This is true for beam energies for above threshold (Fig. 4.7) and for beam energies near threshold (Fig. 4.8).

These results lead to the following conclusion about an electron beam propagating in the atmosphere.

43

As an electron beam propagates upward in the atmosphere, it loss energy and sees a diminishing index of refraction. If the beam radiates over its entire length the effect will be to narrow the radiation cone and diminish the radiation as the diminishing beam propagates upward. If the beam is prevented from radiating by a plasma shield along most of its length, then only the short upper part of the beam would be expected to radiate. In this case, diffraction broadening could be severe, expecially for the lower frequency harmonics of the radiation.

LIST OF REFERENCES

1. Jelly, J. V., _Cerenkov Radiation and Its Applications_, New York, Pergamon Press, 1958.

2. Beach, John B., "Atmospheric Effects on Radio Wave Propagation", _Journal of Defence Electronics Technology_, p.75, Feb., 1980.

3. _U. S. Standard Atmosphere_, pp.40-44, National Oceanic and Atmospheric Administration, 1976.

4. Humphreys, _Physics of the Air_, p.80, McGraw-Hill Book Co. Inc., New York and London, 1940.

5. Allen, C. W., _Astrophysical Quantities_, p.114, Athlone Press, 1973.

6. Naval Postgraduate School Report NPS-61-85-005, _Emission Threshold for Cerenkov Radiation_, by J. R. Neighbours, F. R. Buskirk, and Xavier K., 1 July 1985

7. Buskirk F. R. and Neighbours J. R., "Electron Beam Bunch Profile Determination through Cerenkov Radiation" _Physial Review A28_, pp. 1531-38, 1983.

8. Naval Postgraduate School Report NPS-61-84-010, _Diffraction Effects in Cerenkov Radiation_, by J. R. Neighbours and F. R. Buskirk, June 1983.

9. Naval Postgraduate School Report NPS-61-84-007, _Cerenkov Radiation in the Neighborhood of the Emission Threshold_, by F. R. Buskirk and J. R. Neighbours, May 1984.

10. Yoon Dae Choi, _Design Consideration for the X-Ray Cerenkov Experiment_, M. S. Thesis, Naval Postgraduate School, 1984.

11. Tverskoi P. N., _Physics of the Atmosphere_, National Technical Information Service, 1965.

12. List Robert J., _Smithsonian Meteorological Tables_, The Smithsonian Institution, 1951.

13. Gray Dwight E., _American Institute of Physics Handbook_, p.2-137, McGraw-Hill, Third Edition, 1972.

14. "Preliminary Topics on EM Propagation and Index of Refraction", Meteorology Department Handout, Naval Postgraduate School, Monterey, CA, Unpublished.

INITIAL DISTRIBUTION LIST

		No.	Copies
1.	Library,Code 0142 Naval Postgraduate School Monterey, Califonia 93943-5000		2
2.	Defense Technical Information Center Cameron Station Alexandria, Virginia 22304-6145		2
3.	Chairman, Code 61 Department of Physics Naval Postgradute School Monterey California 93943-5100		1
4.	Professor J. R. Neighbours, Code 61Nb Department of Physics Naval Postgradute School Monterey California 93943-5100		3
5.	Professor F. R. Buskirk, Code 61Bs Department of Physics Naval Postgradute School Monterey California 93943-5100		3
6.	Library Korea Military Academy Gong-reung-Dong 556-21 Republic of Korea 360		1
7.	JOO, Kyung Ro 31/8, 250-52, Go Chuk Dong Young Dung Po Gu, Seoul Republic of Korea		3
8.	Kim, Young Ok 368, 1-Ga, Song Chun-Dong, Jhon Ju, Jhon Book, Seoul Korea, 520-00		3
9.	Yim, Chang Ho SMC 2425 Naval Postgradute School Monterey California 93943		1
10.	Yoon, Seog Koo SMC 2426 Naval Postgradute School Monterey California 93943		1

END

FILMED

3-86

DTIC